Journal of Fluorine Chemistry 130 (2009) 755–758

Contents lists available at ScienceDirect

Journal of Fluorine Chemistry

journal homepage: www.elsevier.com/locate/fluor

Synthesis and upconversion luminescence properties of Yb^{3+}/Tm^{3+}-codoped $BaSiF_6$ nanorods

Guofeng Wang [a,b], Weiping Qin [a,*], Daisheng Zhang [a,c], Guodong Wei [a], Kezhi Zheng [a], Lili Wang [a], Fuheng Ding [a]

[a] State Key Laboratory on Integrated Optoelectronics, College of Electronic Science and Engineering, Jilin University, Changchun 130012, PR China
[b] Department of Chemistry, Tsinghua University, Beijing 100084, PR China
[c] College of Physics, Beihua University, Jilin 132011, PR China

ARTICLE INFO

Article history:
Received 7 January 2009
Received in revised form 7 May 2009
Accepted 15 May 2009
Available online 23 May 2009

PACS:
78.66.J
82.80.C

Keywords:
Rare earth
Nanorods
Upconversion
Luminescence

ABSTRACT

One-dimensional $BaSiF_6$:Yb^{3+}(20%)/Tm^{3+}(1.2%) nanorods were synthesized by a facile microemulsion method for the first time. X-ray topographic analysis found that the nanorods have a pure rhombohedral structure. Under 980 nm excitation, bright-blue upconversion luminescence was presented in the nanorods, indicating that $BaSiF_6$ is a new host material for producing desirable upconversion luminescence.

1. Introduction

During the past decade, one-dimensional nanostructures (such as nanowires, nanotubes, nanobelts, and nanorods) have received steadily growing interests due to their potential applications in fabricating nano-electronic and nano-optoelectronic devices [1–5]. Compared to their bulk counterparts, nanomaterials are expected to possess novel physical properties resulting from the quantum effects and a high surface-to-volume ratio [6–9].

Among the nanomaterials reported, fluoride nanocrystals have aroused great interest because fluorides are efficient host matrix for luminescent centers due to their low phonon energies and optical transparency over a wide wavelength range [10–19]. Especially, fluoride-based upconversion (UC) materials, which can present UC from infrared to ultraviolet/visible light by converting multiple lower-frequency photons into one higher-frequency photon, have shown great potential for use in information technology, data storage, color displays, biological labelling, and so on [7–24]. However, the external UC efficiency is usually no more than 1% in Tm^{3+}-containing systems [25]. Therefore, how to increase the UC emission intensities has become one hot topic of optical functional materials in recent years. Many studies have indicated that the UC luminescence properties of nanocrystals doped with rare earth (RE) ions are very sensitive to their shape and size, which set off a new upsurge of synthesizing fluoride nanocrystals with desirable morphologies [22,23]. For example, Sun et al. synthesized $NaYF_4$:Yb^{3+}/Er^{3+} nanocrystals with different shapes and investigated their UC luminescence properties [24]; Ritcey et al. synthesized YF_3 nanoparticles with hexagonal and quadrilateral shape [26]; Li et al. synthesized LaF_3 nanoplates [27]. However, as a fluorescent host, $BaSiF_6$ has seldom been investigated except for Pr^{3+} doped $BaSiF_6$ powder reported by Kolk et al. [28]. In this paper, $BaSiF_6$:Yb^{3+}/Tm^{3+} nanorods were synthesized by microemulsion method for the first time. Pumped with a 980-nm diode laser, bright-blue UC luminescence from the nanorods was observed.

2. Results and discussion

The XRD patterns of the nanorods (before and after aging) are presented in Fig. 1. All of the diffraction peaks can be readily

* Corresponding author at: State Key Laboratory on Integrated Optoelectronics, College of Electronic Science and Engineering, Jilin University, 2699 Qianjin Street, Changchun 130012, PR China.
E-mail address: wpqin@jlu.edu.cn (W. Qin).

0022-1139/$ – see front matter © 2009 Elsevier B.V. All rights reserved.
doi:10.1016/j.jfluchem.2009.05.013

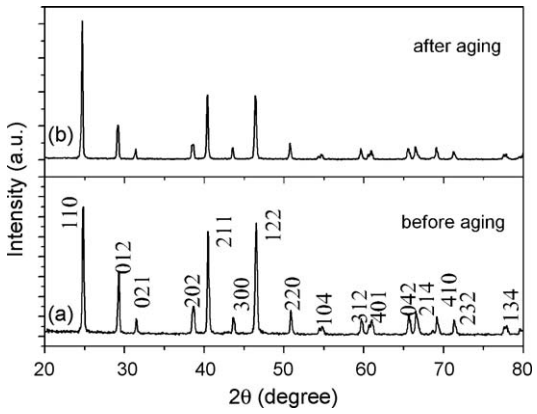

Fig. 1. XRD pattern of the nanorods.

indexed to those of rhombohedral $BaSiF_6$ (ICDD Card No. 15-0736). No other impurity peaks were detected. The crystal data and Rietveld refinement result of nanorods are shown in Table 1.

The morphology of the nanocrystals was characterized by TEM observations (Fig. 2), which clearly reveal a rod-like nanostructure. The nanorods are ~1 μm in length and ~100 nm in diameter. The electron diffraction pattern (inset to Fig. 2b) reveals that the nanorods are single-phased crystals and also stable enough to withstand the irradiation of convergent high-energy electron beam. The electron diffraction pattern of the nanorod after aging (inset to Fig. 2c) is similar to that of the product before aging. According to the reported growth mechanism of YF_3 nanocrystals forming in the quaternary reverse microemulsion system [15–17], the whole growth process of $BaSiF_6$ nanorods should comprise two major steps: (1) nucleation and formation of primary particles; and (2) formation of final products. To verify the validity of the growth mechanism, $BaSiF_6$ nanorods aged for 7 days were investigated (Fig. 2c). From the TEM data of nanorods before aging, we can see that nanorods may be the aggregation of many small nanoparticles. The nanorods after aging most likely have grown from the aggregated small nanoparticles. Of course, $BaSiF_6$ and YF_3 nanocrystals have different final morphology although they were synthesized by the same method ($BaSiF_6$ nanocrystals are rod-like and YF_3 nanocrystals are bundle-like) [17]. We suggest that this can be attributed to the different crystal structure of $BaSiF_6$ and YF_3 nanocrystals. Here, $BaSiF_6$ is rhombohedral and YF_3 is orthorhombic. Rhombohedral phase structure might be benefit for the formation of nanorods and orthorhombic phase structure might be benefit for the formation of nanbundles, on which no final conclusion has yet been reached.

Fig. 3 shows the UC luminescence spectra of $BaSiF_6$:Yb^{3+}(20%)/Tm^{3+}(1.2%) nanorods (before and after aging) under 980 nm excitation (~220 W/cm^2), which present the characteristic emissions of Tm^{3+} ions. The emissions come from the following transitions: $^1D_2 \rightarrow {}^3H_6$ (~363 nm), $^1D_2 \rightarrow {}^3F_4$ (~457 nm), $^1G_4 \rightarrow {}^3H_6$ (~477 nm), $^1G_4 \rightarrow {}^3F_4$ (~646 nm), $^3F_2 \rightarrow {}^3H_6$ (~678 nm), $^3F_3 \rightarrow {}^3H_6$ (~697 nm), and $^3H_4 \rightarrow {}^3H_6$ (~797 nm). The UC luminescence difference of samples is closely related to the shapes, sizes, and crystallinity of nanocrystals.

Table 1
Crystal data and Rietveld refinement result of nanorods.

Symmetry	Rhombohedral
Space group	$R\bar{3}m$ (166)
Calculated cell parameters (nm)	a = 7.19, c = 7.02
Calculated volume of a unit cell (Å^3)	314.15
Calculated density (g cm^{-1})	4.4309
Number of refined parameters	21
Reliability factors (R-factor)	R_P = 0.108, R_{WP} = 0.121

Compared to the fluorides reported [18–20], such as YF_3:Yb^{3+}/Tm^{3+}, the $BaSiF_6$:Yb^{3+}/Tm^{3+} nanorods have different UC luminescence properties, which can be attributed to the difference of phase structure of them. As mentioned above, YF_3 is orthorhombic phase and $BaSiF_6$ is rhombohedral phase. The trivalent Yb^{3+}/Tm^{3+} substitutes for trivalent Y^{3+} ion in YF_3:Yb^{3+}/Tm^{3+} and substitutes for the divalent Ba^{2+} ion in $BaSiF_6$:Yb^{3+}/Tm^{3+}. The YF_3 crystal structure (Z = 4) belongs to space group *Pnma* (62). The positions of the four Y^{3+} are the same in either space group. Each Y^{3+} has eight F^- neighbors at about 2.3 Å, and another at 2.60 Å. The coordination should be described as 8-fold, because of the greater distances to the ninth neighbor [30]. The $BaSiF_6$ crystal structure belongs to space group $R\bar{3}m$ (166) with one type of Ba-atom at a site of D_{3d} point symmetry. Ba is coordinated by 12 F^- ions at an average distance of 282.9 pm. The small Si^{4+} atoms are coordinated octahedrally by 6 F^- ions [29]. Furthermore, the fluorides reported were heated or pressurized, such as hydrothermal treatment and annealing. Here, although $BaSiF_6$:Yb^{3+}/Tm^{3+} nanorods were not conventionally heated or pressurized, bright-blue upconversion luminescence was still observed under 980 nm excitation, indicating that $BaSiF_6$:Yb^{3+}/Tm^{3+} is a new UC luminescence material.

To investigate the fundamental UC mechanism of $BaSiF_6$:Yb^{3+}/Tm^{3+} nanorods, the dependence of pumping power on the fluorescent intensities was investigated. For an unsaturated UC process, the emission intensity is proportional to the n-th power of the excitation intensity, and the integer n is the number of the laser photons absorbed per upconverted photon emitted [31]. Fig. 4 shows the power dependence of the UC emission intensities: n = 3.8, 2.7, and 1.9 for the 363, 477, and 797 nm emissions, respectively. This means that the population of the states $^1D_2$, $^1G_4$, and $^3H_4$ came from four-photon, three-photon, and two-photon UC processes, respectively.

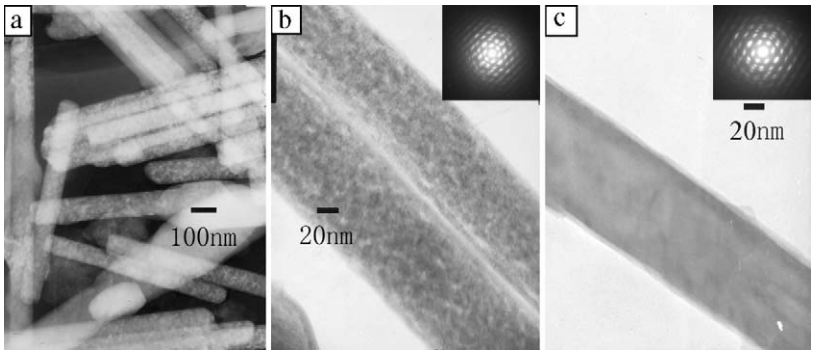

Fig. 2. (a) TEM image of $BaSiF_6$ nanorods before aging. (b) Magnified TEM image and electron diffraction pattern of $BaSiF_6$ nanorods before aging. (c) TEM image and electron diffraction pattern of $BaSiF_6$ nanorods aged for 7 days.

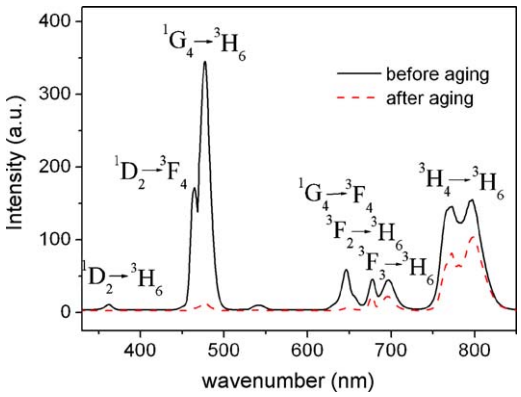

Fig. 3. UC emission spectrum of $BaSiF_6$:Yb^{3+}(20%)/Tm^{3+}(1.2%) nanorods.

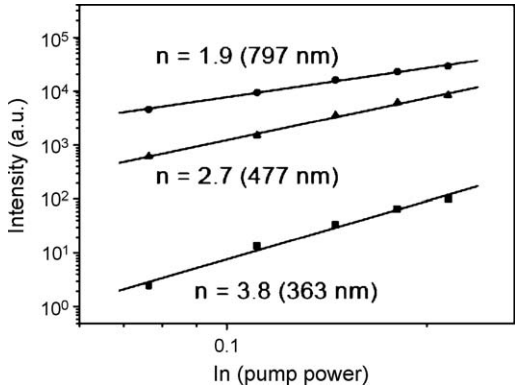

Fig. 4. Dependence of the UC emission intensities on the excitation power.

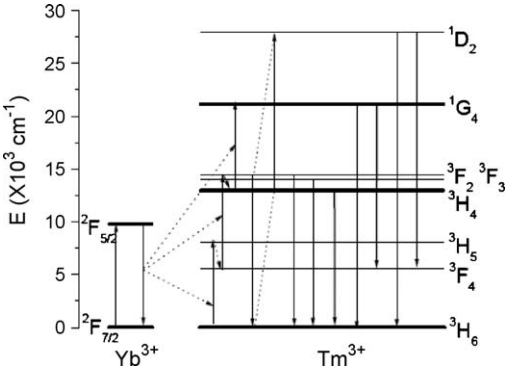

Fig. 5. Schematic diagram of Yb^{3+}-sensitized Tm^{3+} UC in $BaSiF_6$:Yb^{3+}/Tm^{3+} nanorods.

The energy level diagrams of Tm^{3+} and Yb^{3+} ions as well as the UC mechanism are presented in Fig. 5. The pump light excites only the Yb^{3+} ions, and three successive energy transfers from Yb^{3+} to Tm^{3+} populate $^3H_5$, $^3F_2$, and $^1G_4$ levels. The $^1D_2$ level of Tm^{3+} cannot be populated by the fourth photon from Yb^{3+} via energy transfer to the $^1G_4$ due to the large energy mismatch (about 3500 cm^{-1}) between them [32]. The cross-relaxation process of $^3F_2 + {}^3H_4 \rightarrow {}^3H_6 + {}^1D_2$ between Tm^{3+} ions may alternatively play an important role in populating $^1D_2$ level [33].

To study the effect of shapes and sizes of $BaSiF_6$:Yb^{3+}/Tm^{3+} nanocrystals on UV UC emissions, different $BaSiF_6$:Yb^{3+}/Tm^{3+} nanocrystals with the same dopant concentrations were synthesized. The UC luminescence spectra and corresponding TEM images of $BaSiF_6$:Yb^{3+}/Tm^{3+} nanocrystals with different morphologies are shown in Fig. S1 in Supporting Information Obviously, the blue UC emissions from nanorods (see Fig. 3) are much strong than those from the nanocrystals presented in Fig. S1. All of these are closely related to the shapes, sizes, and crystallinity of nanocrystals. Theoretically, the local structure of Yb^{3+}/Tm^{3+} in $BaSiF_6$ with different morphologies can be reflected by the emission intensity ratio of $^1D_2 \rightarrow {}^3F_4$ to $^1D_2 \rightarrow {}^3H_6$ [17]. However, the $^1D_2 \rightarrow {}^3H_6$ transition is hardly detected, and thus the change of local structure cannot be further determined.

3. Conclusion

In conclusion, a new infrared-to-visible UC material, Yb^{3+}/Tm^{3+}-codoped $BaSiF_6$ nanorods, was synthesized for the first time. XRD analysis indicates that the nanorods have a pure rhombohedral structure. Under 980 nm excitation, the nanorods presented a bright-blue UC luminescence. The dependence of excitation power on the fluorescence indicated that the population of the states $^1D_2$, $^1G_4$, and $^3H_4$ came from four-photon, three-photon, and two-photon UC processes, respectively.

4. Experimental

In a typical synthesis, two identical solutions, denoted as microemulsions I and II, were prepared by dissolving 2.25 g of CTAB in 50 mL of cyclohexane and 2.5 mL of 1-pentanol. The two microemulsions were separately stirred for 30 min, and then 2 mL of 0.5 M chloride ($BaCl_2$, $YbCl_3$, and $TmCl_3$) aqueous solution and 2 mL of 10% H_2SiF_6 aqueous solution were added dropwise to microemulsions I and II, respectively. After vigorously stirring for 1 h, the two transparent microemulsion solutions were mixed and stirred for another 10 min. The resulting product was immediately collected and washed several times with ethanol and deionized water. Finally, the $BaSiF_6$ nanorods were obtained after the sample was centrifuged and dried in a vacuum at room temperature.

The crystal structures and phase purity of the product were examined by a Rigaku RU-200b X-ray powder diffractomerer (XRD) using a nickel-filtered Cu Ka radiation (λ = 1.5418 Å) in the range of $20^\circ \leq 2\theta \leq 80^\circ$. The size and morphology of the nanorods were investigated by transmission electron microscopy (TEM, JEM 2010 with operating voltage of 200 kV). The UC fluorescence spectrum was recorded with a Hitachi F-4500 fluorescence spectrophotometer under 980 nm excitation.

Acknowledgement

This research was supported by Natural Science Foundation of China (Grant Nos. 50672030 and 10874058).

Appendix A. Supplementary data

Supplementary data associated with this article can be found, in the online version, at doi:10.1016/j.jfluchem.2009.05.013.

References

[1] Z. Yuan, W. Zhou, B. Su, Chem. Commun. 11 (2002) 1023–1202.
[2] Y. Li, X. Li, R. He, J. Zhu, A. Deng, J. Am. Chem. Soc. 124 (2002) 1411–1416.
[3] J. Liu, X. Wang, Q. Peng, Y. Li, Adv. Mater. 17 (2005) 764–767.
[4] X. Li, Q. Peng, J. Yi, X. Wang, Y. Li, Chem. Eur. J. 12 (2006) 2383–2391.
[5] J. Liang, Y. Li, J. Cryst. Growth 261 (2004) 577–580.
[6] X. Bai, H. Song, L. Yu, L. Yang, Z. Liu, G. Pan, S. Lu, X. Ren, Y. Lei, L. Fan, J. Phys. Chem. B 109 (2005) 15236–15242.
[7] X. Bai, H. Song, G. Pan, Y. Lei, T. Wang, X. Ren, S. Lu, B. Dong, Q. Dai, L. Fan, J. Phys. Chem. C 111 (2007) 13611–13617.
[8] Z. Hou, P. Yang, C. Li, L. Wang, H. Lian, Z. Quan, J. Lin, Chem. Mater. 20 (2008) 6686–6696.
[9] J. Yang, C. Li, Z. Cheng, X. Zhang, Z. Quan, C. Zhang, J. Lin, J. Phys. Chem. C 111 (2007) 18148–18154.

[10] C. Li, J. Yang, P. Yang, H. Lian, J. Lin, Chem. Mater. 20 (2008) 4317–4326.
[11] C. Li, J. Yang, Z. Quan, P. Yang, D. Kong, J. Lin, Chem. Mater. 19 (2007) 4933–4942.
[12] C. Li, Z. Quan, P. Yang, J. Yang, H. Lian, J. Lin, J. Mater. Chem. 18 (2008) 1353–1361.
[13] C. Li, Z. Quan, J. Yang, P. Yang, J. Lin, Inorg. Chem. 46 (2007) 6329–6337.
[14] Y. Jin, W. Qin, J. Zhang, J. Fluorine Chem. 129 (2008) 515–518.
[15] G. Wang, W. Qin, Y. Xu, L. Wang, G. Wei, P. Zhu, R. Kim, J. Fluorine Chem. 129 (2008) 1110–1113.
[16] G. Wang, W. Qin, J. Zhang, J. Zhang, Y. Wang, C. Cao, L. Wang, G. Wei, P. Zhu, P. Kim, J. Fluorine Chem. 129 (2008) 621–624.
[17] G. Wang, W. Qin, J. Zhang, J. Zhang, Y. Wang, C. Cao, L. Wang, G. Wei, P. Zhu, R. Kim, J. Phys. Chem. C 112 (2008) 12161–12167.
[18] R. Yan, Y. Li, Adv. Funct. Mater. 15 (2005) 763–770.
[19] G. De, W. Qin, J. Zhang, J. Zhang, Y. Wang, C. Cao, Y. Cui, J. Lumin. 122 (2007) 128–130.
[20] G. De, W. Qin, J. Zhang, D. Zhao, J. Zhang, Chem. Lett. 34 (2005) 1–3.
[21] Y. Wang, W. Qin, J. Zhang, C. Cao, J. Zhang, Y. Jin, P. Zhu, G. Wei, G. Wang, L. Wang, Chem. Lett. 36 (2007) 1–3.
[22] M. Wang, Q. Huang, H. Zhong, X. Chen, Z. Xue, X. You, Cryst. Growth Des. 7 (2007) 2106–2111.
[23] F. Tao, Z. Wang, L. Yao, W. Cai, X. Li, Growth Des. 7 (2007) 854–858.
[24] Y. Sun, Y. Chen, L. Tian, Y. Yu, X. Kong, J. Zhao, H. Zhang, Nanotechnology 18 (2007) 275609/1–275609/9.
[25] Y. Mita, Y. Wang, Appl. Phys. Lett. 62 (2004) 802–804.
[26] J. Lemyre, A. Ritcey, Chem. Mater. 17 (2005) 3040–3043.
[27] C. Li, X. Liu, P. Yang, C. Zhang, H. Lian, J. Lin, J. Phys. Chem. C 112 (2008) 2904–2910.
[28] E. van der Kolk, P. Dorenbos, C. van Eijk, A. Vink, C. Fouassier, F. Guillen, J. Lumin. 97 (2002) 212–223.
[29] B. Hoskins, A. Linden, P. Mulvaney, Inorg. Chim. Acta 88 (1984) 217–222.
[30] Z. Zalkin, D. Templeton, J. Am. Chem. Soc. 75 (1953) 2453–2458.
[31] M. Pollnau, D. Gamelin, S. Lüdel, Phys. Rev. B 61 (2000) 3337–3346.
[32] J. Zhang, W. Qin, J. Zhang, Y. Wang, C. Cao, Y. Jin, G. Wei, G. Wang, L. Wang, J. Nanosci. Nanotechnol. 8 (2007) 1–4.
[33] G. Qin, W. Qin, C. Wu, S. Huang, Solid State Commun. 125 (2003) 377–380.